Multi-channel Measurement-based Identification Methods for Mode Estimation in Power Systems

Eleftherios O. Kontis, Iraklis S. Avgitidis, Theofilos A. Papadopoulos, Georgios A. Barzegkar-Ntovom, Grigoris K. Papagiannis

***Abstract*-- Mode identification from post-disturbance ringdown responses is a valuable tool for the analysis of the dynamic performance and the stability margins of power systems. In this aspect, several techniques have been proposed, focusing mainly to single-signal analysis. However, considering large-scale power systems and especially future scenarios with high penetration of distributed energy resources, detailed network analysis at all voltage levels is required. As a result of these concerns, multi-channel mode identification algorithms have been developed. Scope of this paper is to evaluate the applicability and the performance of the most known multi-channel measurement-based identification approaches for the modal analysis of modern power systems incorporating active distribution networks. The algorithmic details and distinct characteristics of each method are briefly discussed. The examined methods are used to identify the dominant inter-area modes contained in ringdown responses at different levels of a combined transmission-distribution network.**

***Keywords*: Matrix pencil, mode estimation, multi-signal analysis, power system dynamics, Prony, vector fitting.**

I. Introduction

VITAL information regarding grid oscillations and stability margins of the power system can be provided by mode estimation, i.e., the mode frequency (f) and damping factor (σ) [1] - [3]. In this context, nowadays, online identification techniques are constantly used due to the increasing deployment of synchronized measurement technologies at power systems and the development of wide-area monitoring systems (WAMS), enabling the close to real-time estimation of oscillatory modes [4].

Originally, mode identification entails the analysis of system responses as single entities (single-channel approach). To obtain representative mode estimates of the overall system rather than of specific parts, multi-channel techniques have been introduced to process a set of measured signals [5]. The added information of the multi-channel approach enables more accurate estimates and facilitates mode classification to inter-area and local [6]. The existing multi-channel techniques estimate the modal properties in one of two ways.

The first is based upon estimating a set of coefficients, assumed to be common for each of the measured signals, by analyzing multiple signals simultaneously, i.e., in terms of multi-signal fitting. In most cases, this involves the solution of an overdetermined set of equations. For the analysis of oscillatory ringdown events, several multi-signal techniques have been proposed. The most known is based on Prony analysis [6]. Since then, the multi-signal Prony method has been also employed in several other works improving [7] or extending its applicability [8]. Multi-signal estimation algorithms have been also established by means of the Fourier transform [9] and relevant modifications [10]. Other multi-signal estimation algorithms include the matrix pencil (MP) [11], vector-fitting (VF) [12], [13], autoregressive moving average exogenous (ARMAX) models [14], multi-dimensional wavelets [15] and dynamic mode decomposition [16] for the analysis of oscillatory modes in transmission networks (TNs).

In the second approach, single-channel analysis is applied independently to each of the available signals and the modal estimates are derived. These estimates are grouped, based on the corresponding mode frequency; for each group the final modal estimates are obtained by applying the arithmetic mean or weighted averaging [17] - [19].

Scope of the paper is to systematically evaluate the performance of different multi-channel measurement-based identification techniques for the analysis of oscillatory modes. The contributions of the paper are: a) a comparative analysis between single- and multi-channel approaches is performed. For this purpose, single- and multi-channel implementations of Prony, VF, and MP methods are developed and analyzed. The analysis is applied to a combined transmission-active distribution network (ADN) to investigate mode propagation as well as the applicability of multi-signal architectures for analysis of complex TN - ADN interactions [20]. In all examined cases, multi-channel implementations outperform the corresponding single-channel counterparts. b) The performance of three distinct multi-channel approaches is evaluated and quantified. In the first approach, single-channel analysis is applied to several signals and mode estimates are derived by means of arithmetic mean. In the second approach, instead of arithmetic mean, weighted averaging is applied

The research work was supported by the Hellenic Foundation for Research and Innovation (H.F.R.I.) under the "First Call for H.F.R.I. Research Projects to support Faculty members and Researchers and the procurement of highcost research equipment grant" (Project Number: HFRI-FM17-229).

E. O. Kontis, I. S. Augitidis and G. K. Papagiannis are with the School of Electrical and Computer Engineering, Aristotle University of Thessaloniki, Thessaloniki 54124, Greece (e-mail: ekontis@ece.auth.gr, heraclesavg@gmail.com, grigoris@eng.auth.gr).

T. A. Papadopoulos and G. A. Barzegkar-Ntovom are with the Power Systems Laboratory, Department of Electrical and Computer Engineering, Democritus University of Thrace, Xanthi 67100, Greece (e-mail: thpapad@ee.duth.gr, gbarzegk@ee.duth.gr).

E. O. Kontis is also with the Department of Electrical and Computer Engineering, University of Western Macedonia, Kozani, 50100, Greece.

Paper submitted to the International Conference on Power Systems Transients (IPST2021) in Belo Horizonte, Brazil June 6-10, 2021.

using the mode energy as the weighting factor. In the third approach, multiple signals are processed simultaneously, and mode estimates are derived by solving the overdetermined sets of equations. The accuracy and computational performance of the examined multi-channel implementations are quantified under different conditions using responses from the TN and the ADN. The conducted analysis reveals that the third approach provides the most accurate mode estimates. To the authors best knowledge, a systematic comparison of the above-mentioned multi-channel implementations is presented for the first time in the archived literature.

The rest of the paper is organized as follows: In Section II, the single- and multi-channel implementations of Prony, MP, and VF techniques are mathematically described. In Section III, the procedure used to evaluate the examined methods is discussed. Numerical results are presented in Section IV. In particular, the performance of the different methods is evaluated using frequency and voltage dynamic responses acquired from a TN as well as an ADN. The impact of noise on the accuracy of the examined methods is evaluated and the computational burden of the developed multi-channel implementations is quantified. Finally, Section V summarizes research remarks, proposes topics for future research and concludes the paper.

II. Multi-channel Ringdown Responses

Power systems are nonlinear, complex and time-varying. However, ringdown responses $y(t)$ of the nonlinear system can be approximated by a sum of N damped sinusoids [1]

$$\hat{y}(t)=\sum_{i=1}^{N} A_i e^{\sigma_i t}\cos(\omega_i t+\varphi_i),\ i=1\ldots N \tag{1}$$

where $\hat{y}(t)$ is the estimated response and A_i, φ_i and $\lambda_i=\sigma_i \pm j\omega_i$ the amplitude, phase and eigenvalues, respectively; ω_i, σ_i is the mode angular frequency and the damping factor [1]. Assuming the signal is sampled at period T_s, (1) is written in z-domain [21]

$$\hat{y}[n]=\hat{y}[nT_s]=\sum_{i=1}^{N} c_i z_i^n,\ n=1\ldots N_w-1 \tag{2}$$

where $c_i=A_i\cdot e^{\pm j\varphi_i}/2$ is the mode residue, $z_i=e^{\lambda_i T_s}$ and N_w is the total number of the samples. Alternatively, in terms of transfer function representation, the Laplace transform $Y(s)$ of (1) is used; $Y(s)$ is a rational function expressed by

$$Y(s)=\sum_{i=1}^{N}\frac{c_i}{s-p_i} \tag{3}$$

where each pole p_i is associated to eigenvalue λ_i.

In case a set of M ringdown signals $y_m(t)$ is available, $m\in[1,M]$, that share the same set of eigenvalues λ_i, (2) can be rewritten in generalized form as

$$\hat{y}_m[n]=\hat{y}_m[nT_s]=\sum_{i=1}^{N} c_{mi} z_i^n \tag{4}$$

where $c_{mi}\in\mathbf{C}$.

A. Prony Analysis

The most known method to identify the unknown parameters of (2) is by means of Prony analysis [21]; it is assumed that $\hat{y}[n]$ satisfies the auto-regressive sequence

$$\hat{y}[nT_s]=b_1\hat{y}[(n-1)T_s]+\ldots+b_N\hat{y}[(n-N)T_s] \tag{5}$$

with characteristic polynomial

$$d(z)=1-\left(b_1 z^{-1}+b_2 z^{-2}+\ldots+b_n z^{-N}\right). \tag{6}$$

The unknown coefficients b_i are calculated by means of a linear prediction model. In this sense, the roots z_i of $d(z)$ are determined and related with the system eigenvalues λ_i; the associated residues c_i are determined by compiling (5) into a Vandermonde matrix form and solve the system.

In the multi-signal case, the linear prediction problem of (5) is formulated as [6]

$$\hat{y}_m[nT_s]=b_1\hat{y}_m[(n-1)T_s]+\ldots+b_N\hat{y}_m[(n-N)T_s]. \tag{7}$$

The unknown coefficients of the system are simultaneously solved in the same sense as in the single-channel case; the residues of the signals are calculated individually.

B. Matrix Pencil

Considering a single dynamic response, MP adopts singular value decomposition (SVD) to estimate the actual system modes [22]. Initially, Hankel matrices $\mathbf{H}_0$ and $\mathbf{H}_1$ with entries the samples of the system response are constructed. In particular, $\mathbf{H}_0$ is defined as

$$\mathbf{H}_0=\mathbf{PSQ}^T \tag{8}$$

where $\mathbf{P}$ and $\mathbf{Q}$ are singular vector matrices and $\mathbf{S}$ is a diagonal matrix of singular values. SVD is applied on $\mathbf{H}_0$ and the system order is determined by retaining the largest singular values. Vectors $\mathbf{V}_1$ and $\mathbf{V}_2$ are constructed by deleting the last and the first row of the unitary vector $\mathbf{V}_N$, respectively; the elements of $\mathbf{V}_N$ correspond to the most significant values of $\mathbf{S}$. By using $\mathbf{V}_1$ and $\mathbf{V}_2$ the matrices $\mathbf{Y}_1$ and $\mathbf{Y}_2$ are calculated as

$$\mathbf{Y}_1=\mathbf{V}_1^T\mathbf{V}_1 \tag{9}$$

$$\mathbf{Y}_2=\mathbf{V}_2^T\mathbf{V}_1. \tag{10}$$

The signal modes are the eigenvalues of the matrix pair $\{\mathbf{Y}_2; \mathbf{Y}_1\}$, resulting from

$$\mathbf{Y}_1^{-1}\mathbf{Y}_2 - \lambda\mathbf{I}. \quad (11)$$

The residues are calculated by means of (5), similarly to Prony method.

The MP method can be extended to utilize multiple signals by constructing the Hankel matrices $\mathbf{H}_0^M$ and $\mathbf{H}_1^M$ for each of the M signals and concatenate vertically the resulting $\mathbf{H}_0^M$ matrices into a single matrix $\mathbf{H}_0'$ as follows [11]

$$\mathbf{H}_0' = \begin{bmatrix} \mathbf{H}_0^1 & \mathbf{H}_0^2 & \cdots & \mathbf{H}_0^M \end{bmatrix}^T. \quad (12)$$

The algorithm proceeds similarly as for the single signal case, by applying SVD to $\mathbf{H}_0'$. The resulting matrices are used to estimate λ_i by introducing them into (11); the residues of each signal are calculated similarly as in Prony method.

C. Vector Fitting

Given $Y(s)$ by applying e.g., the fast Fourier transform, VF can approximate (3) on the basis of a two-stage linear least squares problem [23], by determining the poles contained in the ringdown [24]. In the first step, VF relocates a set of initial pole estimates to better positions by solving (13) with the known poles $\alpha_k^{(r)}$; r denotes the r-th iteration.

$$\underbrace{\left(\sum_{k=1}^{N}\frac{\tilde{r}_k^{(r)}}{s-\alpha_k^{(r)}}+\tilde{d}^{(r)}\right)}_{\sigma'^{(r)}(s)}Y(s) \cong \underbrace{\sum_{k=1}^{N}\frac{r_k^{(r)}}{s-\alpha_k^{(r)}}+r_0^{(r)}}_{\sigma' Y^{(r)}(s)}. \quad (13)$$

The poles p_i of $Y(s)$ are calculated by solving the eigenvalue problem of

$$\tilde{\mathbf{z}}^{(r)} = \boldsymbol{\alpha}^{(r+1)} = eig\left(\mathbf{A}^{(r)} - \mathbf{b}^{(r)}\tilde{d}^{-1(r)}\mathbf{c}^{T(r)}\right) \quad (14)$$

where $\tilde{z}_k^{(r)}$ are the zeros of $\sigma'^{(r)}(s)$, $\tilde{d}^{(r)}$ is scalar and matrices $\mathbf{A}^{(r)}$, $\mathbf{b}^{(r)}$ and $\mathbf{c}^{(r)}$ are defined by the rational model of $\sigma'^{(r)}(s)$. By replacing the poles with the new ones, an improved set is achieved until $\alpha_k^{(r)}$ tends to p_i. The second step applies to calculate the unknown residues by using (14), assuming $\sigma'^{(r)}(s)$ equal to unity.

Apart from single-channel responses, VF is eminently suited to process simultaneously several responses assuming a common set of poles [25]. The main objective is to collect the M frequency responses $\hat{Y}_m(s)$ of $\hat{y}_m[n]$ into a single vector $\mathbf{Y}(s) \in \mathbf{C}^M$ and compute the common set of poles for all components of the vector model. Therefore, the unknown parameters are calculated following the two-step procedure of the basic VF algorithm. The pole relocation iteration is performed in order to find the model poles in terms of (13) for all components and for all frequencies. In the second step the residues and r_0 are determined.

D. Weighted Averaging

All above multi-channel analysis algorithms combine the M signals to derive a common formulation and compute simultaneously a common set of poles. Another approach is to apply the mode estimation algorithm individually to each of the M signals; the derived modes from each signal are grouped based on the corresponding mode frequency. The task of computing the final estimate of the mode frequency $\overline{f_i}$ and the damping factor $\overline{\sigma_i}$ for each group of modes is formulated as a weighted averaging problem as shown in (15) and (16), respectively,

$$\overline{f_i} = \sum_{m=1}^{M}\frac{w_i^m}{\sum_{m=1}^{M} w_i^m}\hat{f}_i^m \quad (15)$$

$$\overline{\sigma_i} = \sum_{m=1}^{M}\frac{w_i^m}{\sum_{m=1}^{M} w_i^m}\hat{\sigma}_i^\ell \quad (16)$$

where w_i^m is the weighting factor of the i-th mode for the m-th signal. The weighting factor can be set equal to the corresponding mode energy $E_i^m = 1/2\left(\omega_i A_i^m\right)^2$ [17], [18] or for ease of simplicity equal to unity, reducing the weighted averaging problem to an arithmetic mean.

III. Evaluation Procedure

In this Section, the procedure used to evaluate the performance of the examined multi-channel analysis techniques is presented.

A. System Under Study

For the analysis, a modified benchmark power system is used. The modified test system is implemented in DIgSILENT and it is comprised of a high voltage (HV) TN and a medium voltage (MV) ADN. The TN is the "Two-area Kundur test system" [26] and the ADN is based on the benchmark European MV network proposed by CIGRE [27]. A single-line diagram of the examined system is presented in Fig. 1.

The Kundur system is a 230 kV, 60 Hz TN, containing two areas, connected by a weak tie between buses T7 and T9. Two loads and two shunt capacitors are connected to buses T7 and T9. The test system contains also four synchronous generators (SGs) with identical control systems. SGs are modeled using the sixth order model. They are equipped with IEEE 1S excitation system, IEEE Type 2 speed-governing

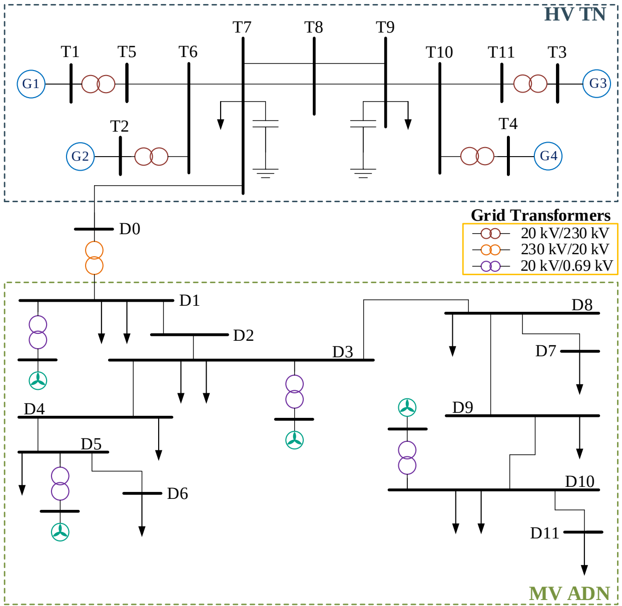

Fig. 1. Examined power system.

model, and speed sensitive power system stabilizer. Further information concerning the modeling of SGs are given in [28].

The CIGRE European MV distribution grid is a 20 kV, 50 Hz system, containing two discrete feeders. To achieve an interconnection with the Kundur system, all reference values are modified to apply to 60 Hz. The first feeder of the MV grid is connected at Bus T7 of the TN via a 230/20 kV transformer. The second feeder is omitted in the presented analysis. All MV grid switches are considered open. All MV loads are modeled as constant impedance loads; their rated power can be found in [27]. Additionally, four distributed generators (DGs) are connected to buses D1, D3, D5 and D10 of the MV grid. All DGs are connected to the grid via full scale power converters and are modeled using the Type 4a model [29].

B. *Simulated Events*

To evaluate the accuracy of the examined multi-channel techniques, the following procedure is adopted: Initially, two discrete ringdown events are generated by performing RMS simulations with the full nonlinear model of the system, depicted in Fig. 1. Afterwards, ringdown responses are processed and forwarded as inputs to the examined techniques to estimate the inter-area mode of the test system. Details concerning the considered ringdown events and the processing of the dynamic responses are provided in the next paragraphs.

The first ringdown event (*RE*#1) is generated by disconnecting one of the two lines connecting buses T7 and T8. The disconnection occurs at t = 1s. The line is reconnected at t = 2s. Ringdown responses of frequency signals are acquired from all buses that host SGs and DGs. The second ringdown event (*RE*#2) is generated by simulating a three-phase short circuit (SC). The SC is applied to bus T8 at t = 1s. The fault impedance is considered equal to 1 Ω and the fault duration is 10 cycles. In this ringdown event, responses of voltage signals are recorded. The data acquisition rate for both events is set to 100 samples per second. Frequency responses, recorded during *RE*#1, are depicted in Fig. 2, while voltage responses, recorded during *RE*#2, are illustrated in Fig. 3.

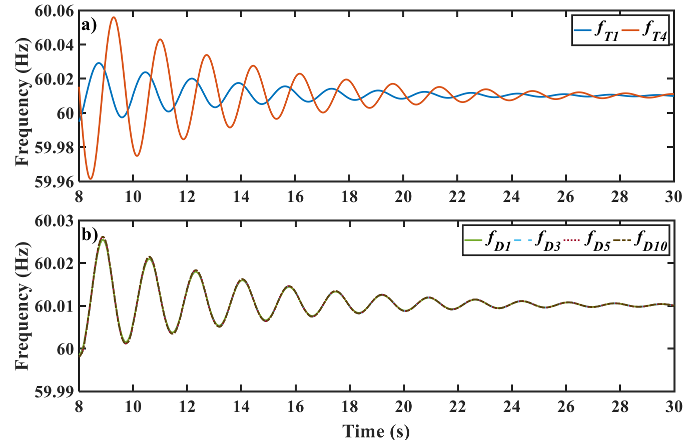

Fig. 2. Time-domain responses of frequency signals acquired during *RE*#1. Responses recorded from a) TN and b) ADN buses.

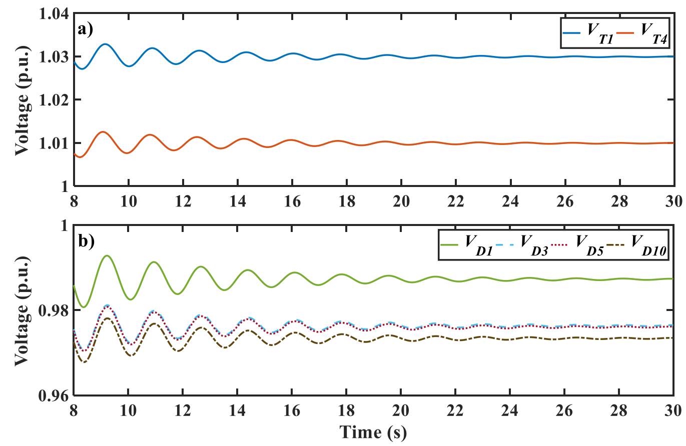

Fig. 3. Time-domain responses of voltage signals acquired during *RE*#2. Responses recorded from a) TN and b) ADN buses.

Responses of Fig. 2 and Fig. 3 are distorted with additive white Gaussian noise (AWGN) to replicate real field conditions. Responses acquired at TN buses are distorted assuming a signal to noise ratio (SNR) equal to 30 dB; responses acquired at ADN buses are distorted with SNR equal to 15 dB, since in distribution networks, higher noise levels are usually reported [4], [30].

To investigate statistically the performance of the examined multi-channel techniques, the Monte Carlo (MC) method is applied and a group of 100 data sets is generated for each ringdown event. MCs are used to represent discrete instances of noise [6]. Noisy responses are detrended to remove the mean component of the signals and filtered using a low pass filter of order 15 and cut-off frequency equal to 10 Hz. The filtered signals are then used as inputs to the examined methods to estimate the inter-area mode. The analysis timeframe is from t = 8s to t = 30s. The analysis does not start immediately after the reconnection of the line to eliminate nonlinearities and fast-damped modes, thus achieving better accuracy in the inter-area estimates [31].

The performance of the examined multi-channel techniques is assessed by comparing the estimated inter-area mode with the corresponding system eigenvalue, computed using the linear model of the test system. The eigen-analysis reveals that the inter-area mode has a frequency equal to 0.5811 Hz and a damping factor equal to -0.1588 s^{-1}, i.e., λ=-0,1588 + 2π0,5811. To fully quantify modal estimation errors, the median absolute deviation (*MAD*) is used [4]

$$MAD = median(|\lambda_i - \lambda|). \tag{17}$$

Here, λ_i denotes the mode estimate of the *i*-th MC simulation and λ is the actual inter-area mode. Note that, *MAD* value equal to zero denotes a perfect modal estimate.

IV. Numerical Results

In the next subsections, two cases are considered. Initially, the inter-area mode is determined using signals recorded at different buses of the TN. For this purpose, signals depicted in Fig. 2a and Fig. 3a are used. As shown in Fig. 2a, generator G1 oscillates against generator G4. Single-signal analysis, using responses acquired from only one generator, will result in varying mode estimates; thus, being very difficult for the user to determine the accurate ones. In this case, multi-signal analysis can be a valuable tool, since it can be used to analyze both signals to obtain one "optimum" common mode value.

Afterwards, the inter-area mode is determined using signals recorded at different buses of the ADN. For this analysis, the signals of Fig. 2b and Fig. 3b are used. As shown, all signals recorded from ADN buses oscillate with the same frequency. Therefore, single-channel analysis will theoretically result in the same estimates for the inter-area mode. However, in highly noisy environments, the single-channel analysis may lead to erroneous estimates. On the other hand, the multi-signal analysis can effectively filter out the negative impact of noise, resulting in more accurate and robust estimates.

A. Multi-channel analysis using TN Responses

Initially, ringdown frequency responses, recorded at buses T1 and T4 of the TN during *RE*#1, are used to estimate the inter-area mode. These responses are denoted as f_{T1} and f_{T4}. Initially, f_{T1} and f_{T4} are analyzed separately by applying the Prony and MP methods to the time-domain signal; concerning VF the spectrum of the ringdown is fitted [24]. To develop models of minimum order (minimum required number of artificial modes to fit the distorted response [4]) and to ensure a common comparative base in the analysis, a fourth order approximation is used for all methods. The resulting *MAD* error for all MC simulations is presented in Fig. 4 by means of boxplots. As shown, single-channel analysis results in varying mode estimates. This is more pronounced for Prony.

Therefore, to derive more accurate mode estimates, three multi-channel analysis techniques are tested. In the first approach, single-channel analysis is conducted in f_{T1} and f_{T4} using Prony, VF and MP methods. Afterwards, for each method the arithmetic mean of the mode estimates is derived. This approach is denoted for the rest of the paper as AM. In the second approach, instead of using simple arithmetic mean, weighted averaging is applied, assuming as weighting factor

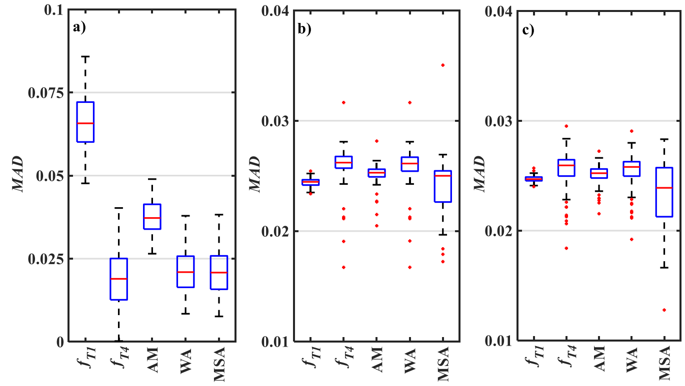

Fig. 4. MAD errors for a) Prony, b) VF and c) MP. The analysis is performed using ringdown frequency responses recorded from TN buses during *RE*#1.

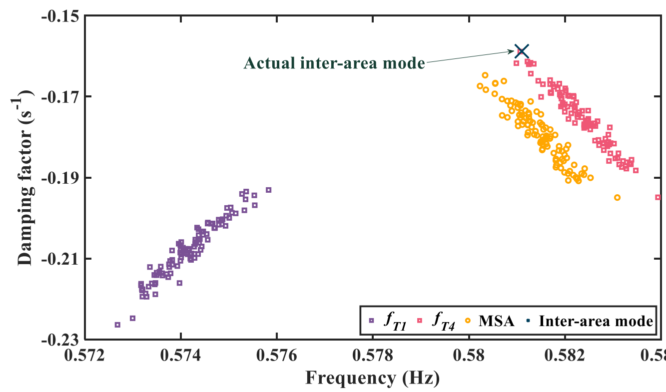

Fig. 5. Variability of mode estimates; single- and multi-signal Prony analysis.

the mode energy. This approach is denoted as WA. Finally, the multi-signal implementations of Prony, VF and MP are tested. In these implementations, all signals are processed simultaneously and a common set of mode estimates is derived for each method. This approach is referred for the rest of the paper as multi-signal analysis (MSA).

As shown, in Fig. 4, the performance of the three examined identification methods is enhanced using multi-channel analysis. Indeed, in all cases, erroneous estimates, derived from single-channel analysis, are efficiently cancelled out and lower *MAD* error is obtained following the multi-channel analysis. Among the examined multi-channel approaches, the MSA provides the most accurate results.

To further highlight the importance of multi-channel analysis, the mode estimates derived using Prony analysis through the 100 MC are plotted in Fig. 5. As shown, by applying single-channel analysis to frequency responses acquired from T1, erroneous estimates are derived. Indeed, the mode frequency varies from 0.5725 Hz to 0.576 Hz and mode damping from -0.23 s^{-1} to -0.19 s^{-1}, while the true inter-area mode frequency is 0.5811 Hz and the damping is equal to -0.1588 s^{-1}. Due to these erroneous estimates, the corresponding *MAD* in Fig. 4 is considerably high. The implementation of multi-channel techniques cancels out the erroneous estimates, leading to more accurate results.

The performance of the multi-channel approaches is also assessed using the second dataset, i.e., the ringdown voltage responses obtained during *RE*#2. The corresponding results

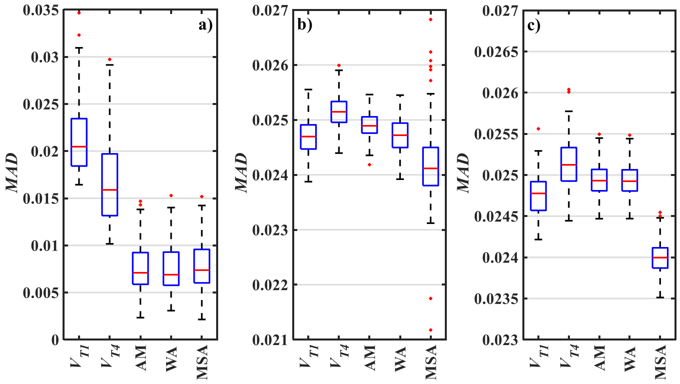

Fig. 6. MAD errors for a) Prony, b) VF and c) MP. The analysis is performed using ringdown voltage responses recorded from TN buses during *RE*#2.

are summarized in Fig. 6. Also, in this dataset, it is verified that the use of the multi-channel approaches enhances the performance of the examined identification techniques.

B. Multi-channel analysis using ADN Responses

In this Section, the performance of the multi-channel implementations is evaluated using ringdown responses acquired at the ADN buses. For this purpose, the inter-area mode is estimated using two datasets. The first dataset contains the ringdown frequency responses recorded during *RE*#1 at buses D1, D3, D5, and D10 of the ADN. These responses are denoted for the rest of the paper as f_{D1}, f_{D3}, f_{D5}, and f_{D10}. The second dataset includes ringdown voltage responses recorded at the same ADN buses during *RE*#2. These responses are denoted as V_{D1}, V_{D3}, V_{D5}, and V_{D10}.

The resulting *MAD* error for the two datasets is summarized in Figs. 7 and 8, respectively. By assessing the results, it is clear that the variability of mode estimates, due to noise, is higher for the single-channel analysis compared to multi-channel approaches. This is also evident from Fig. 9 where the variability of mode estimates using single- and multi-signal VF analysis is analyzed. Considering the above, among the examined methods, Prony results in the highest *MAD* error. VF and MP practically exhibit the same accuracy, leading to *MAD* error four times lower compared to Prony analysis.

The computational burden of the multi-channel implementations is quantified by calculating the required

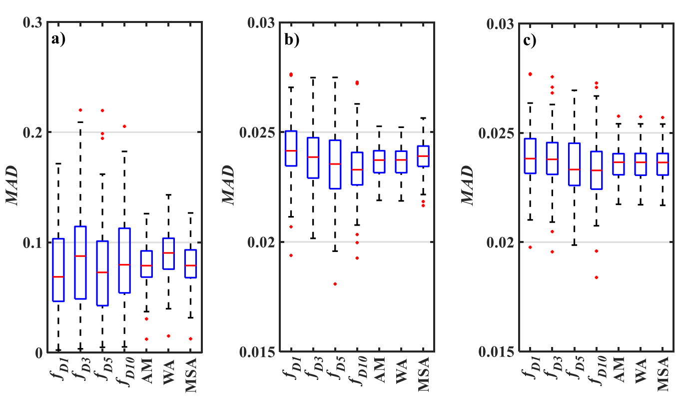

Fig. 7. MAD errors for a) Prony, b) VF and c) MP. The analysis is performed using ringdown frequency responses recorded from ADN buses during *RE*#1.

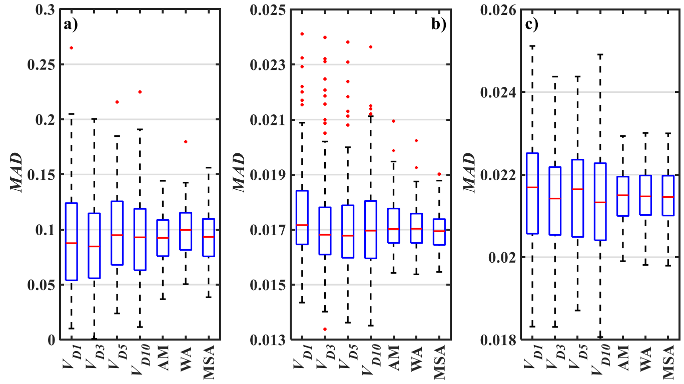

Fig. 8. MAD errors for a) Prony, b) VF and c) MP. The analysis is performed using ringdown voltage responses recorded from ADN buses during *RE*#2.

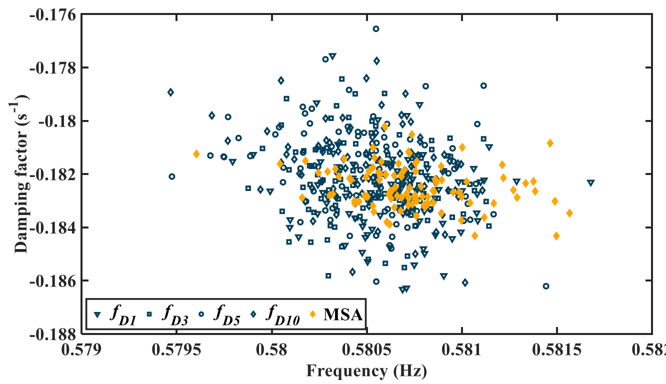

Fig. 9. Variability of mode estimates; single- and multi-signal VF analysis. The analysis is performed using ringdown frequency responses recorded from ADN buses during *RE*#1.

execution time. For this purpose, the 100 MC simulations generated using frequency responses recorded during *RE*#1, are used. The mean execution time for the 100 MC simulations is summarized in Fig. 10. All simulations have been performed using an i9-9900K, 3.6 GHz, 32 GB RAM personal computer. The analysis reveals that the execution time highly depends on the number of the available signals. In the presented analysis, four signals are considered, and the approximation order is set to 4 for all methods. Using these settings, the following remarks can be done: Prony exhibits the lowest computational burden, while MP the highest. Among the examined multi-channel implementations, the MSA approach presents the lowest computational burden.

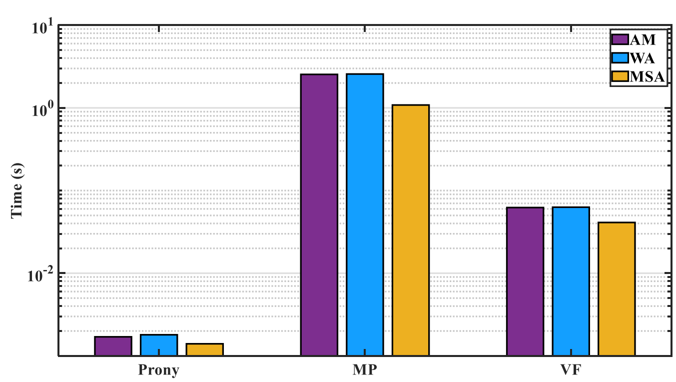

Fig. 10. Computational burden of the examined multi-channel implementations.

Indeed, the execution time for MSA of Prony, VF, and MP is equal to 1.4 ms, 41.1 ms, and 1.2 s, respectively. However, is should be noted that Prony results in considerably higher *MAD* error compared to MP and VF. To increase the accuracy of Prony, higher order approximations must be used [4], [32]. In this case, the execution time of Prony becomes comparable with the execution time of VF method reported in Fig. 10.

AM and WA approaches present higher computational burden compared to the corresponding MSA. This remark can be easily explained. In MSA approach all signals are analyzed simultaneously. On the other hand, in AM and WA approaches each signal is analyzed separately in a sequential manner. Afterwards, mode estimates are derived using arithmetic mean or weighted averaging. The sequential analysis of the available signals increases considerably the required execution time. However, the computational burden of AM and WA approaches can be efficiently reduced by using parallel computing [33]. In this case, the execution time required by AM and WA is 75% lower compared to the execution time reported in Fig. 10. Supporting of parallel computing is an advantage of AM and WA approaches compared to MSA.

Additionally, to investigate the impact of noise on the performance of the examined multi-channel implementations, MC simulations for SNR levels equal to 20 dB, 15 dB and 10 dB are performed. For each SNR level, 100 MCs are generated using the ringdown responses recorded during *RE*#1. Indicative results are presented for MSA and WA approaches in Fig. 11 and Fig. 12, respectively. AM results in *MAD* errors similar to those reported in Fig. 11 and Fig. 12. The analysis reveals that both multi-channel implementations of MP and VF are practically not influenced from the SNR level. On the other hand, noticeable performance degradation is observed for Prony when the SNR level reduces. Note that in case single-signal analysis is applied, Prony results in higher *MAD* error compared to those presented in Fig. 11 and 12. To enhance Prony performance in highly noisy environments, higher order approximations should be used, resulting in increased computational burden.

Finally, to provide a further insight concerning the accuracy of the examined MSA implementations, the cumulative distribution functions (CDFs) of the resulting *MAD* error is illustrated in Fig. 13. In this figure, representative results for SNR = 15 dB are presented.

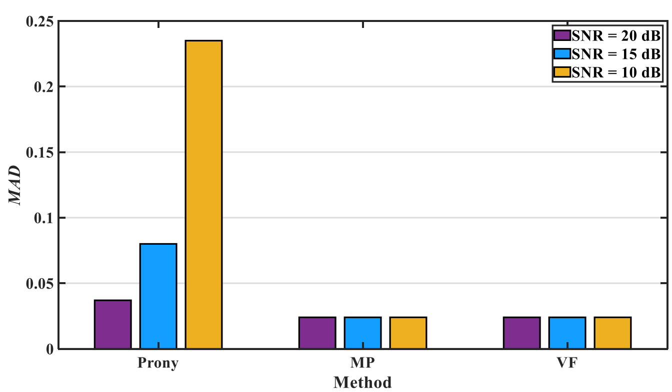

Fig. 11. MAD errors of MSA implementations under different SNR levels.

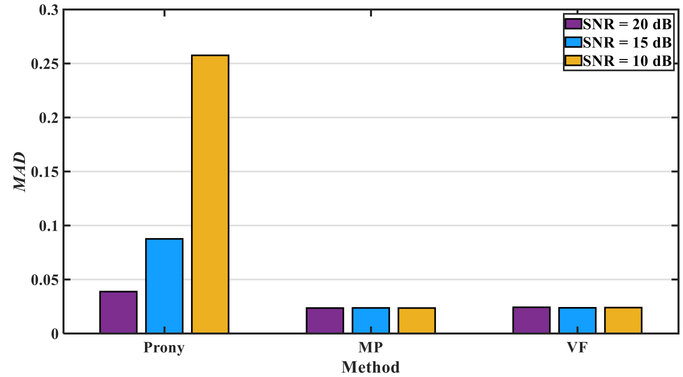

Fig. 12. MAD errors of WA implementations under different SNR levels.

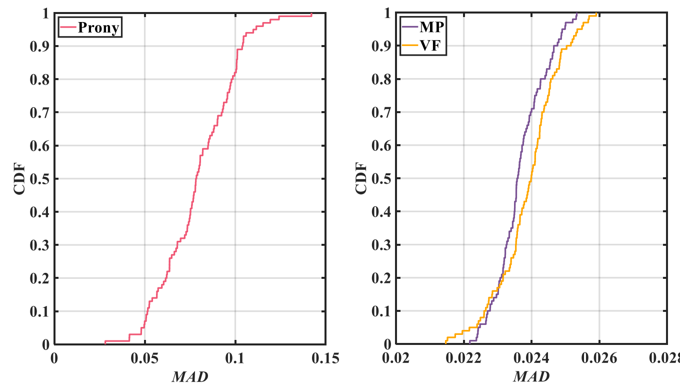

Fig. 13. CDFs of *MAD* errors for MSA implementations. SNR = 15 dB.

In 90% of the examined cases, the MSA implementation of MP and VF provides *MAD* error lower than 0.025. Prony provides in all cases *MAD* error higher than 0.025. In 20% of the cases, Prony results in *MAD* error four times higher compared to those obtained via VF and MP.

V. Conclusions

In this paper, the single-channel formulations of three well-known system identification techniques, namely the Prony, VF, and MP are extended to support multi-channel analysis. The developed multi-channel algorithms are tested to identify the dominant inter-area modes of modern power systems. Their performance is compared with the corresponding single-signal counterparts as well as with two conventional multi-channel approaches that use the arithmetic mean and weighted averaging to determine the dominant system modes.

The analysis is applied on a combined TN-ADN to ensure that the performance of the proposed methods is not affected from complex TN-ADN interactions as well as to investigate mode propagation in ADNs. Results reveal that inter-area modes can be identified using responses either from the TN or ADNs. Multi−channel techniques are more accurate, significantly reducing the impact of noise, canceling out also erroneous mode estimates which may occur using single-channel analysis. Comparisons reveal that the examined multi-channel techniques show in general similar accuracy. However, the MSA approach provides slightly improved mode estimates compared to AM and WA. Among the examined methods, multi-signal implementations of VF and

MP provide the most accurate estimates, resulting in the lowest *MAD* error. The conducted analysis has revealed that the performance of MP and VF multi-channel implementations is practically not affected from the SNR level. On the other hand, Prony method is highly influenced by the noise level.

Among the examined methods, multi-channel implementations of VF are the most suitable for close to real-time applications, since they present low computational burden and high immunity to noise, resulting also in all cases in low *MAD* error. Parallel AM and WA implementations of MP method can also be used for close to real-time applications.

Future work will include systematic investigations on online applicability of the examined multi-channel methods, considering missing data and non-Gaussian measurement error. A monitoring architecture will also be developed based on enhanced MSA methods to support the simultaneous analysis of TN and ADN signals. This will facilitate the analysis of complex TN-ADN interactions.

VI. Acknowledgment

The authors would like to thank K. P. Pippi, and M.E. Dimitriadou for their contributions on the initial study.

VII. References

[1] IEEE task force on identification of electromechanical modes, identification of electromechanical modes in power systems. *IEEE Power & Energy Society*, 2012, PES-TR15, Available: http://resourcecenter.ieee-pes.org.

[2] N. Zhou, J. W. Pierre and D. Trudnowski, "A Stepwise Regression Method for Estimating Dominant Electromechanical Modes," IEEE Trans. Power Syst., vol. 27, no. 2, pp. 1051-1059, 2012.

[3] J. J. Sanchez-Gasca and J. H. Chow, "Performance comparison of three identification methods for the analysis of electromechanical oscillations," IEEE Trans. Power Syst., vol. 14, no. 3, pp. 995-1002, 1999.

[4] E. O. Kontis, T. A. Papadopoulos, G. A. Barzegkar-Ntovom, A. I. Chrysochos, G. K. Papagiannis, "Modal analysis of active distribution networks using system identification techniques," *Int. J. Electr. Power Energy Syst.*, vol. 100, pp. 365-378, 2018.

[5] Luke Dosiek, John W. Pierre, "Multichannel Techniques for the Estimation of Power System Electromechanical Modes," *IFAC Proceedings Volumes*, vol. 45, Issue 16, pp. 1013-1018, 2012

[6] D. J. Trudnowski, J. M. Johnson and J. F. Hauer, "Making Prony analysis more accurate using multiple signals," *IEEE Trans. Power Syst.*, vol. 14, no. 1, pp. 226-231, 1999.

[7] M. Netto and L. Mili, "Robust Data Filtering for Estimating Electromechanical Modes of Oscillation via the Multichannel Prony Method," *IEEE Trans. Power Syst.*, vol. 33, no. 4, pp. 4134-4143, 2018.

[8] S. Zhao and K. A. Loparo, "Forward and Backward Extended Prony (FBEP) Method for Power System Small-Signal Stability Analysis," *IEEE Trans. Power Syst.*, vol. 32, no. 5, pp. 3618-3626, 2017.

[9] Z. Tashman, H. Khalilinia and V. Venkatasubramanian, "Multi-Dimensional Fourier Ringdown Analysis for Power Systems Using Synchrophasors," *IEEE Trans. Power Syst.*, vol. 29, no. 2, pp. 731-741, 2014.

[10] Alejandro Zamora, V. Mani Venkatasubramanian, José Antonio de la O Serna, Juan M. Ramirez, M.R.A. Paternina, "Multi-dimensional ringdown modal analysis by filtering," Electr. Power Syst. Res., vol. 143, pp. 748-759, 2017.

[11] W. Trinh, K.S. Shetye, I. Idehen, T.J. Overbye, "Iterative Matrix Pencil Method for Power System Modal Analysis," *Proceedings of the 52nd Hawaii International Conference on System Sciences*, 2019.

[12] E.S. Bañuelos-Cabral, J.J. Nuño-Ayón, B. Gustavsen, J.A. Gutiérrez-Robles, V.A. Galván-Sánchez, J. Sotelo-Castañón, J.L. García-Sánchez, "Spectral fitting approach to estimate electromechanical oscillation modes and mode shapes by using vector fitting," Electr. Power Syst. Res., vol. 176, 2019.

[13] R. Schumacher, G.H.C. Oliveira, R. Kuiava, "A multi-signal instrumental variable vector fitting method for estimating inter-area electromechanical modes of power systems," *Int. J. Electr. Power Energy Syst.*, vol. 111, pp. 1-13, 2019.

[14] L. Dosiek and J. W. Pierre, "Estimating electromechanical modes and mode shapes using the multichannel ARMAX model," *IEEE Trans. Power Syst.*, vol. 28, no. 2, pp. 1950-1959, 2013.

[15] X. Pan and V. Venkatasubramanian, "Multi-dimensional wavelet analysis for power system oscillation monitoring using synchrophasors," *2012 IEEE PES Innovative Smart Grid Technologies (ISGT)*, Washington, DC, 2012, pp. 1-10.

[16] E. Barocio, B. C. Pal, N. F. Thornhill and A. R. Messina, "A Dynamic Mode Decomposition Framework for Global Power System Oscillation Analysis," *IEEE Trans. Power Syst.*, vol. 30, no. 6, pp. 2902-2912, 2015.

[17] J. Ning, X. Pan and V. Venkatasubramanian, "Oscillation modal analysis from ambient synchrophasor data using distributed frequency domain optimization," IEEE Trans. Power Syst., vol. 28, no. 2, pp. 1960-1968, 2013.

[18] J. Ning, S. A. N. Sarmadi and V. Venkatasubramanian, "Two-Level Ambient Oscillation Modal Estimation from Synchrophasor Measurements," *IEEE Trans. Power Syst.*, vol. 30, no. 6, pp. 2913-2922, 2015.

[19] M. R. Arrieta Paternina, R. Kumar Tripathy, A. Zamora-Mendez, D. Dotta, "Identification of electromechanical oscillatory modes based on variational mode decomposition," Electr. Power Syst. Res., vol. 167, Pages 71-85, 2019.

[20] F. Escobar, J. García, J. M. Víquez, G. Valverde, P. Aristidou, "A Combined High-, Medium-, and Low-Voltage Test System for Stability Studies with DERs," *Electr. Power Syst. Res.*, vol. 189, 106671, 2020.

[21] J. F. Hauer, C.J. Demeure, L.L. Sharf, "Initial results in Prony analysis of power system response signals," *IEEE Trans. Power Syst.*, vol. 5, no.1, pp.80-89, Feb. 1990.

[22] Y. Hua, T. Sarkar, "Matrix pencil method for estimating parameters of exponentially damped/undamped sinusoids in noise," *IEEE Trans. Acoust. Speech and Sign. Proc.*, vol. 38, no. 5, pp.814-824, May 1990.

[23] B. Gustavsen, A. Semlyen, "Rational approximation of frequency domain responses by vector fitting," *IEEE Trans. Power Deliv.*, vol. 3, 1261-1267, 2000.

[24] T. A. Papadopoulos, A. I. Chrysochos, E. O. Kontis, G. K. Papagiannis, "Ringdown analysis of power systems using vector fitting," *Electr. Power Syst. Res.*, vol. 141, 2016, pp. 100-103.

[25] S. Grivet-Talocia, B. Gustavsen, "Passive Macromodeling: Theory and Applications," John Wiley & Sons, Incorporated, 2016.

[26] P. Kundur, "Power system stability and control," New York, London, McGraw-Hill, 1994, p. 1176.

[27] CIGRE Task Force C6.04.02, "Benchmark systems for network integration of renewable and distributed energy resources," Technical report, CIGRE, 2014.

[28] F. Gonzalez-Longatt, J. L. Rueda Torres, "Advanced smart grid functionalities based on PowerFactory," Green and Energy Technology, Springer, 2018.

[29] IEC Wind Energy Generation Systems – Part 27-1: Electrical Simulations Models – Generic Models, 2020.

[30] J. K. Hwang and Y. Liu, "Noise Analysis of Power System Frequency Estimated from Angle Difference of Discrete Fourier Transform Coefficient," IEEE Trans. Power Del., vol. 29, no. 4, pp. 1533-1541, Aug. 2014.

[31] T. A. Papadopoulos, A. I. Chrysochos, E. O. Kontis, P. N. Papadopoulos and G. K. Papagiannis, "Measurement-Based Hybrid Approach for Ringdown Analysis of Power Systems," IEEE Trans. Power Syst., vol. 31, no. 6, pp. 4435-4446, Nov. 2016.

[32] Meng Jia, N. Zhou and B. G. Amidan, "A comparative study on the Prony analysis and the ERA for modal analysis," *2016 IEEE Power and Energy Society General Meeting (PESGM)*, Boston, MA, 2016, pp. 1-5.

[33] P. Saraf, G. Kumar Venayagamoorthy and B. Luitel, "Online oscillation monitoring of synchronous generators using Parallel-Prony analysis," *ISGT 2014*, Washington, DC, 2014, pp. 1-5.